

Heparan Sulfate Proteoglycans Control Intracellular Processing of bFGF in Vascular Smooth Muscle Cells[†]

Gizette V. Sperinde and Matthew A. Nugent*

Departments of Biochemistry and Ophthalmology, Boston University School of Medicine, Boston, Massachusetts 02118

Received March 16, 1998; Revised Manuscript Received June 29, 1998

ABSTRACT: Basic fibroblast growth factor (bFGF) is a potent mitogen for vascular smooth muscle cells (VSMC) and has been implicated in a number of vascular disorders. bFGF interacts with high-affinity receptors and heparan sulfate proteoglycans (HSPG) at the cell surface. HSPG have been demonstrated to enhance bFGF binding to its receptors, yet no known role for HSPG in modulating postbinding events has been identified. In the present study, we analyzed bFGF internalization, intracellular distribution, degradation, and stimulation of DNA synthesis within native and HSPG-deficient VSMC. HSPG-deficient VSMC were generated by treating cells with sodium chlorate to inhibit the sulfation of HSPG. We found that stimulation of DNA synthesis by bFGF in chlorate-treated VSMC was markedly reduced as compared with native cells, even at doses of bFGF where receptor binding was similar in the two conditions. This was not a general lack of mitogenic potential, as the addition of calf serum, or epidermal growth factor, stimulated DNA synthesis to a similar extent in native and chlorate-treated cells. Analysis of the accumulation of internalized bFGF within cytoplasmic and nuclear fractions of native and HSPG-deficient VSMC showed striking differences. At early time points (0–2 h), nearly identical amounts of bFGF were observed in the cytoplasmic fractions under both conditions, yet significant amounts of bFGF were only found in the nuclear fractions of native cells. At later time points (2–48 h), the amount of cytoplasmic bFGF was significantly greater in the native compared to HSPG-deficient cells, and nuclear deposition of bFGF began to reach similar levels under both conditions. Furthermore, the intracellular half-life of bFGF was dramatically prolonged in native compared to HSPG-deficient cells, in part, due to decreased bFGF degradation in native cells. Thus, HSPG appears to accelerate nuclear localization, increase cytoplasmic capacity, and inhibit intracellular degradation of bFGF in VSMC. Modulation of intracellular processing of bFGF by HSPG might control the biological activity of bFGF in VSMC.

Basic fibroblast growth factor (bFGF)¹ is a prototypical member of a family of at least nine related polypeptides. bFGF induces pleiotropic effects in a variety of cell types (1). These responses range from induction of cell differentiation in neuronal cells (2), to inhibition of differentiation in skeletal muscle cells (3), to stimulation of proliferation in many cell types including vascular smooth muscle cells (1, 4–7). At the cell surface, bFGF binds to tyrosine kinase receptors, as well as to heparan sulfate proteoglycans (HSPG)

(8–10). The FGF receptor family consists of four gene products. Alternative splicing of the message gives rise to many isoforms of receptors which can have different affinities for the various members of the FGF family. FGF receptors (FGFR) have been shown to have tyrosine kinase activity, leading to activation of the mitogen-activated protein kinase and phospholipase C- γ signal transduction pathways (9). Furthermore, several recent studies have suggested that FGF receptors might have additional signaling functions once internalized from the cell surface (11, 12). Maher (11) has shown that FGF receptors are translocated to the nucleus in response to bFGF, and Prudovsky et al. (12) have observed increased tyrosine kinase activity in peri-nuclear fractions of cells treated with aFGF.

HSPG consist of a protein core and at least one heparan sulfate side chain (13). bFGF binds the heparan sulfate moieties of the HSPG. It has been shown that sulfation of the heparan sulfate chains is required for the binding of bFGF to these molecules (14–16). Cell-associated HSPG also modulate the activity of FGF at a number of levels (10, 17, 18). HSPG have been shown to increase the affinity of bFGF for its receptor at the cell surface, by lowering the rate at which it dissociates from its receptor, suggesting that bFGF, its receptor, and HSPG form a ternary complex on the cell

[†] This work was supported in part by Grants RO1HL56200 and P01HL46902 from the National Institutes of Health, American Heart Association Grant-in-Aid 13-522-923, a Whitaker Foundation Biomedical Engineering Research grant, and departmental grants from the Massachusetts Lions Eye Research Fund and Research to Prevent Blindness, Inc.

* Correspondence should be addressed to this author at the Department of Biochemistry, Room K225, Boston University School of Medicine, 715 Albany St., Boston, MA 02118. Fax: 617 638-5339. E-mail: nugent@med-biochem.bu.edu.

¹ Abbreviations: bFGF, basic fibroblast growth factor; DCS, dialyzed calf serum; DMEM, Dulbecco's modified Eagle's medium; EGF, epidermal growth factor; GAG, glycosaminoglycans; HSPG, heparan sulfate proteoglycans; K_d , equilibrium dissociation constant; k_{deg} , degradation rate constant; k_{on} , association rate constant; k_{off} , dissociation rate constant; PAO, phenyl arsine oxide; PBS, phosphate-buffered saline; PAGE, polyacrylamide gel electrophoresis; PCNA, proliferating cells nuclear antigen; TCA, trichloroacetic acid; SE, standard error about the mean; VSMC, vascular smooth muscle cells.

surface (18–21). The binding of bFGF to large HSPG in solution or in the extracellular matrix has been shown to protect bFGF from degradation and sequester it from the cell surface (17, 22–24). Data have also been presented suggesting that HSPG and FGF receptors target internalized bFGF to different intracellular locations (25), suggesting the possibility that HSPG play intracellular roles in modulating bFGF activity.

The events following the binding of bFGF to its cell surface receptors include internalization as well as lysosomal degradation of both ligand and receptor resulting in down-regulation of FGF receptors. However, a considerable amount of bFGF has been reported to be translocated into the nuclear fraction of various cell types, including vascular endothelial and smooth muscle cells (26–30). It has also been reported that bFGF translocated to the nuclear fraction is subject to lowered levels of degradation (29). Nuclear translocation appears to be cell cycle dependent, occurring in the G1–S transition in these cells, and has been correlated with increased mitogenic activity (28, 29). There have also been several reports of translocation of FGF receptors to or near the nucleus of various cell types (11, 12, 31–33). Together, this information suggests that there might be intracellular roles for bFGF, its receptors, or a complex of this ligand with its receptor.

A clear role for HSPG in modulating the intracellular trafficking of bFGF and its receptor has not been established. Several studies have suggested that HSPG impact the mechanism of internalization and processing of bFGF (25, 34–37). In bovine capillary endothelial cells, bFGF bound to HSPG is rapidly internalized and metabolized (35); however, HSPG appear to have no effect on the initial rate of internalization in these and other cell types (35, 38). Gannon-Zaki et al. (36) observed a saturable internalization process at concentrations of bFGF that bound principally to receptor sites, while a nonsaturable process was observed at higher concentrations of bFGF, where binding was mostly to HSPG. Further, studies using toxin-conjugated bFGF revealed two distinct fates of internalized bFGF depending on its interaction with receptors or HSPG (25).

In the present study, we analyzed bFGF trafficking in vascular smooth muscle cells (VSMC) in the presence and absence of HSPG. VSMC were chosen for these studies since they have been shown to be very sensitive to growth regulation by bFGF, heparin, and HSPG *in vitro* and *in vivo* (6, 7, 22, 39–43). Addition of bFGF stimulates (6, 7), and neutralizing antibodies to bFGF inhibit (44), the proliferation of vascular smooth muscle cells following denudation of arterial endothelium *in vivo*. It has been postulated that the endothelial cells produce factor(s) which inhibit bFGF at a biochemical level (4, 6, 7, 39, 43, 45–48). Indeed, we have recently demonstrated that large, perlecan core protein containing, HSPG species from aortic endothelial cell cultures are potent inhibitors of bFGF binding and activity in VSMC (22). These results suggest that HSPG modulation of bFGF function plays a significant role in regulating VSMC proliferation.

VSMC were treated with sodium chlorate to metabolically inhibit glycosaminoglycan sulfation so that bFGF binding, trafficking, and activity could be quantitatively analyzed in a single cell type in the presence and absence of HSPG. The elimination of HSPG reduced bFGF receptor binding affinity

and resulted in significantly decreased bFGF stimulation of mitogenesis in these cells. The decreased mitogenic activity of bFGF in HSPG-deficient cells was not accounted for solely by the decreased receptor affinity, suggesting that HSPG modulate additional stages of the bFGF pathway. Indeed, we observed significant differences in the amounts and kinetics of bFGF accumulation in the cytoplasmic and nuclear fractions of native and HSPG-deficient VSMC at 37 °C. Nuclear localization was accelerated, cytoplasmic capacity was increased, and intracellular degradation of bFGF was inhibited in native compared to HSPG-deficient VSMC. Modulation of intracellular processing of bFGF by HSPG might play important roles in regulating the biological activity of bFGF in VSMC.

MATERIALS AND METHODS

Materials. Human recombinant bFGF was from Scios-Nova, Inc. (Mountain View, CA).

¹²⁵I-bFGF was prepared by a modification of the Bolton–Hunter procedure (19). This method has been demonstrated to produce active ¹²⁵I-bFGF as determined by its ability to stimulate DNA synthesis in quiescent Balb/c3T3 cells. The specific activity ranged from 80 to 90 $\mu\text{Ci}/\mu\text{g}$. [³⁵S]Sulfate, ¹²⁵I-epidermal growth factor (EGF murine), ¹²⁵I-Bolton–Hunter reagent, and [³H]thymidine were from DuPont NEN (Boston, MA). Sodium chlorate (NaClO₃) was obtained from Fluka (Ronkonkoma, NY). Phenyl arsine oxide (PAO), *p*-nitrophenyl phosphate (PNP), Nonidet P-40 [poly(ethylene glycol)-*p*-isooctylphenyl ether; octylphenoxypolyethoxyethanol], and other reagent grade chemicals were from Sigma (St. Louis, MO).

Cell Culture. Vascular smooth muscle cells (VSMC) were used between passages 4 and 8. VSMC, isolated as described (49), were a generous gift of Drs. Edward Koo and Elazer Edelman, Massachusetts Institute of Technology (Cambridge, MA), and Coriell Cell Repositories (Camden, NJ). Cells were maintained in 75 cm² vented culture flasks (Costar, Cambridge, MA) in Dulbecco's modified Eagle's medium (DMEM-low glucose, Life Technologies, Inc.), supplemented with 20% FBS (Life Technologies, Inc.), penicillin (100 units/mL), streptomycin (100 $\mu\text{g}/\text{mL}$), and glutamine (2 mM). Cell number was determined with a Coulter Counter, or relative cell numbers were determined by acid phosphatase quantitation (50). Briefly, cells were incubated in 0.1 M sodium acetate (pH 5.5), 0.1% Triton X-100, and 10 mM *p*-nitrophenyl phosphate (Sigma 104 phosphatase substrate) for 45 min at 37 °C. The reaction was stopped by the addition of 1 N NaOH, and absorbance was determined at 410 nm with a Shimadzu UV–Vis spectrophotometer.

Chlorate Treatment. To obtain similar cell numbers for native and chlorate-treated VSMC at the end of the chlorate treatment procedure, chlorate-treated cells were plated at a higher initial seeding density. VSMC were plated at 25 000/cm² for native and at 37 500/cm² for chlorate-treated cells in low-glucose DMEM, 0.5% DCS (Sigma), and glutamine (2 mM). Following cell attachment (~4 h), cells were treated either with sodium chlorate (75 mM final concentration) or with an equal volume of PBS. Cells were then incubated for 48 h at 37 °C. The optimal chlorate concentration was determined by assaying [³⁵S]sulfate incorporation into glycosaminoglycan, in the presence of increasing concentrations

Table 1: ^{35}S -Proteoglycan Production by Native and Chlorate-Treated VSMC^a

	media (cpm)	ECM (cpm)	cell surface (cpm)
native	19376 \pm 1437	3255 \pm 51	1560 \pm 131
chlorate treated	71 \pm 7	49 \pm 1	70 \pm 2

^a VSMC were treated for 48 h with and without 75 mM chlorate in the presence of $^{35}\text{SO}_4$ (100 $\mu\text{Ci/mL}$) to metabolically label sulfated proteoglycan. The medium was collected and proteoglycan extracted from the extracellular matrix (ECM) and cell surface. ^{35}S -Proteoglycan was quantitated by cationic nylon filter binding (52). The results represent the average \pm SE of triplicate determinations.

of sodium chlorate. Cells were prepared as described above. At the time of chlorate addition, [^{35}S]sulfate (100 $\mu\text{Ci/mL}$) was also added, and the cells were incubated at 37 °C for 48 h. Sulfated proteoglycans were collected from media, extracellular matrix, and cell surface fractions and quantitated by cationic nylon filtration, as described previously (51–53). Greater than 97% of glycosaminoglycan sulfation was inhibited by 75 mM chlorate in all fractions analyzed (Table 1). The inhibition of ^{125}I -bFGF binding to HSPG sites on the cell surface of VSMC by 75 mM sodium chlorate was comparable to, and in most cases more effective than, enzymatic digestion of GAG moieties by heparinase I. Cell quiescence was verified through propidium iodide staining followed by flow cytometry with FACScan (Becton Dickinson). A total of 90% of native and 96% of chlorate-treated VSMC were in G₀–G₁, with 1% of the cells in S phase. Cell viability was determined by trypan blue exclusion. Greater than 97% of both native and chlorate-treated VSMC were viable.

^{125}I -bFGF Cell Surface Binding. ^{125}I -bFGF binding to VSMC was conducted as previously described (43), with minor modifications. Cells were plated at 50 000 cells/well, in 24 well culture plates (Costar) in DMEM supplemented with 0.5% DCS and glutamine (2 mM). Chlorate treatment was performed as described above, after cell attachment. When the cultures were quiescent, 48 h later, the medium was replaced with 0.5 mM phenyl arsine oxide (PAO) in binding buffer (DMEM, 25 mM HEPES, 0.05% gelatin). PAO is a potent inhibitor of internalization and was used to allow characterization of binding at 37 °C (54, 55). A dose-dependent inhibition of uptake of ^{125}I -bFGF showed that no further inhibition was achieved with concentrations greater than 0.5 mM PAO. Cells were treated with PAO for 20 min and then incubated with ^{125}I -bFGF for various times until 60 min at 37 °C in order to achieve steady-state cell surface binding. At each time point, medium was removed, and the plates were placed on ice. Cells were washed 3 times with ice-cold binding buffer. This was followed by a high-salt wash (20 mM HEPES, 1 M NaCl, pH 7.4) for approximately 10 s and a rinse with PBS, to remove any HSPG-bound ^{125}I -bFGF. Cells were then washed with a high-salt, low-pH buffer (10 mM sodium acetate, 1 M NaCl, pH 5) and PBS, to remove receptor-bound ^{125}I -bFGF. To ascertain that the above treatment removed all surface-bound ^{125}I -bFGF, cells were extracted with 0.1 M sodium phosphate, 0.5% Triton, pH 8.1, and ^{125}I was quantitated. No significant radioactivity was detected in the detergent-extracted cells. The inhibition of internalization by PAO at 37 °C, discussed above, was comparable to the inhibition of internalization observed when the binding reaction was carried out at 4 °C. Cell numbers

for both native and chlorate-treated VSMC were unaffected by the treatment with PAO. Nonspecific binding was determined empirically at four concentrations of ^{125}I -bFGF (0.07, 0.44, 0.66, and 1.11 nM) in the presence of excess unlabeled bFGF (278 nM). Nonspecific binding of ^{125}I -bFGF was found to be negligible at concentrations below 0.55 nM on all fractions analyzed for both native and chlorate-treated VSMC.

Cellular Fractionation. VSMC were plated at either 25 000/cm² for native or 37 500/cm² for chlorate treatment in 12 well culture dishes (Costar) in DMEM supplemented with 0.5% DCS and glutamine, treated with and without chlorate, and incubated for 48 h, as described above. Cells were exposed to ^{125}I -bFGF, at various concentrations, and incubated at 37 °C for the indicated times. After the incubation, cells were washed 3 times with ice-cold binding buffer (DMEM, 25 mM HEPES, 0.05% gelatin). Prior to cellular fractionation, cell surface associated ^{125}I -bFGF was removed, as described above. ^{125}I -bFGF associated with HSPG was released by extraction with a high-salt buffer (20 mM HEPES, 1 M NaCl, pH 7.4; 0.5 mL/well for 5 s), followed by a wash with PBS. ^{125}I -bFGF associated with cell surface receptors was released by extraction with a high-salt/acid buffer (10 mM sodium acetate, 1 M NaCl, pH 5; for 5 min), followed by a wash with PBS. Cells were trypsinized using 0.5 mL of 0.01% trypsin, 0.53 mM EDTA (Life Technologies, Inc.) per well. Trypsinization was stopped by the addition of 50 μL per well of calf serum (Hyclone, UT). Cell suspensions were placed in a Model 235C microcentrifuge (Fisher Scientific, NJ) and centrifuged for 30 s at 10000g. Cell fractionation proceeded through a modification of a previously described procedure (11). Cell pellets were resuspended by briefly vortexing in 200 μL of homogenization buffer (10 mM HEPES, pH 7.9, 10 mM KCl, 0.1 mM EDTA, 0.1 mM EGTA, 1 mM DTT, 0.5 mM PMSF) and incubated on ice for 15 min. After this incubation, 12.5 μL of a 10% Nonidet P-40 solution was added to each tube, and the samples were vortexed vigorously for 10 s. This was followed by another centrifugation, 30 s at 10000g. The supernatant was collected as the cytoplasmic fraction. The crude nuclear pellet was washed 2 additional times by repeating the procedure outlined above. The nuclear pellet was then resuspended in 100 μL of homogenization buffer. Radioactivity in these fractions was quantitated by counting in a Packard Model 5650 gamma counter. Boiling Laemmli sample buffer was added to the fractions obtained for electrophoretic analysis.

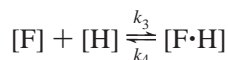
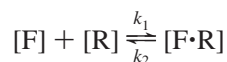
As cell fractionation relies on plasma membrane lysis followed by nuclear separation, we analyzed three separate lysis procedures each followed by two separate separation procedures and found the method described above to be ideal for VSMC based on recovery and quantitation of the lysosomal contaminant, acid phosphatase, in the nuclear fraction (50). Virtually full recovery of the cytoplasmic fraction was observed, based on acid phosphatase quantitation in the cytoplasmic fraction as compared with nonfractionated, whole cells, and less than 0.5% of lysosomal contamination was found in the nuclear fraction using the above procedure. Integrity of the nuclear fractions was confirmed by phase contrast microscopy. We verified that the pellet derived from the fractionation described above contained nuclei. Immunoblot analysis for proliferating cell nuclear antigen (PCNA)

was performed on extracted nuclear fractions from quiescent and proliferating VSMC. PCNA was only present in the nuclear fraction of growing cells. Treatment of native and chlorate-treated VSMC with ^{125}I -EGF, a growth factor which has not been reported to localize to the nucleus of these cells, showed that while EGF can be internalized, it is not found in the nuclear fraction, confirming the fact that contaminating ^{125}I from the cytoplasmic fraction is minimal in the nuclear fraction. To determine whether plasma membrane contamination of ^{125}I in the cytoplasmic and nuclear fractions was significant, equilibrium binding was carried out at 4 °C. Subsequently, cells were subjected to the fractionation described above. We found negligible contamination of ^{125}I in either the cytoplasmic or the nuclear fractions of both native and chlorate-treated VSMC.

Gel Electrophoresis. SDS–polyacrylamide gel electrophoresis (16% running gel, 5% stacking gel) was used to further analyze the degradation pattern of ^{125}I -bFGF collected from cellular fractions. Bio-Rad Prestained SDS–polyacrylamide gel electrophoresis (PAGE) standards were used for molecular mass calibration. ^{125}I -Labeled protein bands were visualized through exposure of the gel onto a phosphorimager SF phosphor plate (Molecular Dynamics).

Western Blot Analyses of FGF Receptor. Native and chlorate-treated cells were rinsed once with PBS. The cells were then solubilized with Laemmli SDS–PAGE sample buffer. Samples were then subjected to 7% SDS–PAGE and electrotransferred to an Immobilon-P membrane (Millipore Corp, Bedford, MA). Membranes were blocked overnight in 5% milk and probed for 1 h at room temperature with a monoclonal antibody to FGF receptor 1 at 1:1000 dilution, followed by 1 h incubation at room temperature with horseradish peroxidase-linked anti-mouse IgG (from sheep) at 1:1000 dilution. Bands were visualized with ECL chemiluminescence (Amersham, LIFE SCIENCE) on Hyperfilm ECL (Amersham, LIFE SCIENCE).

Determination of Binding Constants at 37 °C. To determine the binding rate constants for FGF–receptor binding at 37 °C, the binding data with PAO-treated cells were fit to a computer model. The reactions of binding of bFGF to its cell surface receptors were represented by the following:



where $[\text{F}]$ is the concentration of bFGF in the media, $[\text{R}]$ is the concentration of cell surface high-affinity receptors that are available for binding, $[\text{F}\cdot\text{R}]$ is the concentration of bFGF–receptor complexes at the cell surface, where any bFGF bound to receptor and HSPG simultaneously is included as $[\text{F}\cdot\text{R}]$, $[\text{H}]$ is the concentration of HSPG sites that are available for binding, $[\text{F}\cdot\text{H}]$ is the concentration of bFGF–HS complexes at the cell surface, and k_1 , k_2 , k_3 , and k_4 are the reaction rate constants for the forward (k_1 , k_3) and reverse (k_2 , k_4) binding reactions for the chemical equilibria shown above for bFGF binding to two classes of sites, receptor and HSPG.

For the un-steady-state case of binding at 37 °C, the following differential equations may be written for (eq 1)

bFGF binding to its high-affinity receptors, (eq 2) bFGF binding to its low-affinity receptors, and (eq 3) media depletion of bFGF:

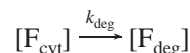
$$\frac{d[\text{F}\cdot\text{R}]}{dt} = k_1[\text{F}][\text{R}] - k_2[\text{F}\cdot\text{R}] \quad (1)$$

$$\frac{d[\text{F}\cdot\text{H}]}{dt} = k_3[\text{F}][\text{H}] - k_4[\text{F}\cdot\text{H}] \quad (2)$$

$$\frac{d[\text{F}]}{dt} = -\frac{d[\text{F}\cdot\text{R}]}{dt} - \frac{d[\text{F}\cdot\text{H}]}{dt} \quad (3)$$

This model assumes uniform binding sites for bFGF on the cell surface, for both the high- and low-affinity receptors. These equations were solved simultaneously and compared with experimental data, to yield kinetic rate constants for the reactions they represent. We used an iterative process, in a computer simulation using FORTRAN on a 100 MHz Think Pad 560 (IBM), which numerically integrates the above equations, given a set of initial reaction rate constants, by a fourth-order Runge Kutta step method. The values derived through the numerical integrator are then compared to experimental data, and the difference (chi squared) is minimized with every iteration. The iterative procedure used continues to change the reaction rate constants until theoretical values are obtained that minimize chi squared. This is done by reguessing for the values of the rate constants through the Levinberg–Marquardt method (56) and reintegrating the equations. The iteration stops when the value of chi squared is within 0.1% of the previously derived chi squared.

Determination of Degradation Constants at 37 °C. The degradation reaction can be represented by



where $[\text{F}_{\text{deg}}]$ is the concentration of degraded bFGF in the media in intact bFGF equivalents, $[\text{F}_{\text{cyt}}]$ is the concentration of bFGF in the cytoplasmic fraction, and k_{deg} is the degradation rate constant.

Equation 4 describes the above reaction:

$$\frac{d[\text{F}_{\text{deg}}]}{dt} = k_{\text{deg}}[\text{F}_{\text{cyt}}] \quad (4)$$

Equation 4 can be integrated to yield eq 5:

$$\int d[\text{F}_{\text{deg}}] = k_{\text{deg}}[\text{F}_{\text{cyt}}] dt \quad (5)$$

which, for experimental data, is estimated as

$$[\text{F}_{\text{deg}}](t) = k_{\text{deg}} \sum [\text{F}_{\text{cyt}}] \Delta t \quad (6)$$

Thus, a plot of the concentrations of degraded bFGF at each time point vs the sum of the cytoplasmic concentrations of bFGF at each time yields a slope, which is equivalent to the k_{deg} . This model treats the cytoplasmic pool of bFGF as a single compartment of the cell. Even though this assumption may not be entirely true, it allows us to observe an apparent k_{deg} which can give comparative information regarding native and HSPG-deficient cells. We have not observed any saturation of this pathway even at high doses of bFGF, which

indicates that observed differences in the apparent k_{deg} for native and chlorate-treated VSMC are not simply due to the fact that native cells are internalizing higher levels of bFGF which they are unable to process.

RESULTS

Off Rate of bFGF Binding to Its Receptors Is Significantly Increased in HSPG-Deficient Cells at 37 °C. Receptor binding of bFGF has been shown to correlate with mitogenic activity in many cell types (8, 38, 57–59). However, these studies have generally involved predicting receptor occupancy levels based on equilibrium binding parameters determined at 4 °C. To evaluate the relationship of bFGF receptor occupancy to biological activity under various conditions, a better understanding of the kinetics of bFGF binding at physiological temperatures is required.

In the present study, we evaluated the role of HSPG in modulating the kinetics of bFGF binding to its cell surface receptors at 37 °C in VSMC. HSPG-deficient VSMC were generated by exhaustive treatment with sodium chlorate. To isolate the cell surface binding reaction at 37 °C, native and chlorate-treated VSMC were exposed to phenyl arsine oxide (PAO) for 20 min, to inhibit internalization of bFGF. The association kinetics of ^{125}I -bFGF with its receptors were measured until steady state was achieved (Figure 1). The apparent forward and reverse binding rate constants were then determined by fitting these data, along with the measured values of free bFGF in the media and bFGF bound to HSPG sites, to a computer model. The kinetics of bFGF receptor binding were significantly different under the two conditions. This was revealed as a 20-fold increase in the apparent off rate constant (k_{off}) in chlorate-treated cells compared to untreated native cells [$k_{\text{off}}(\text{native}) = 0.038 \text{ min}^{-1}$, $k_{\text{off}}(\text{chlorate}) = 0.79 \text{ min}^{-1}$]. The apparent on rate constant (k_{on}) was also increased in chlorate-treated cells, but to a lesser extent [$k_{\text{on}}(\text{native}) = 1.2 \times 10^8 \text{ M}^{-1} \text{ min}^{-1}$; $k_{\text{on}}(\text{chlorate}) = 4.2 \times 10^8 \text{ M}^{-1} \text{ min}^{-1}$] (Table 2). The increased rate of dissociation of bFGF–receptor complexes on chlorate-treated cells resulted in a more rapid approach to steady state in these cells compared to native cells. However, the concentration of occupied receptors was lower in chlorate-treated cells as compared with native VSMC at steady state as indicated by the increase in the dissociation binding constant (Table 2). The decreased level of bFGF binding in chlorate-treated cells was apparent over a wide range of bFGF concentrations with the difference being less pronounced at very high bFGF concentrations as saturation is approached under both conditions (data not shown). To evaluate the total level of FGF receptor expression directly, immunoblot analyses were conducted with anti-FGF-R1 (Figure 2). A single immunoreactive band with an apparent molecular mass of 110 kDa was present in lanes containing native and chlorate-treated cell extracts. There was no significant difference in the levels of FGF receptor expression in native and chlorate-treated cells. Thus, decreased binding of bFGF on chlorate-treated cells was the result of the altered binding kinetics and not a reflection of a change in receptor number.

bFGF Stimulation of DNA Synthesis in HSPG-Deficient VSMC Is Significantly Reduced. It has been shown, in Balb/c3T3 cells, that a decrease in FGF receptor affinity under

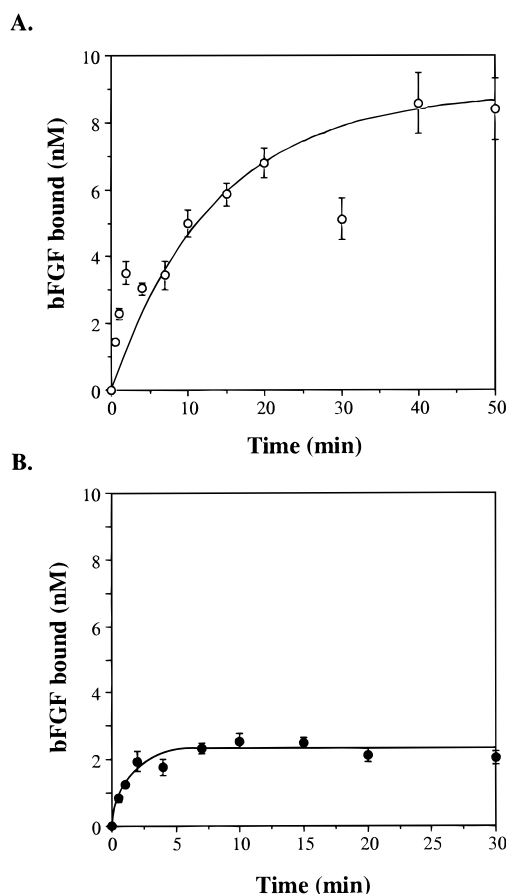


FIGURE 1: Kinetics of ^{125}I -bFGF receptor binding at 37 °C. VSMC were treated with (●) (B) or without (○) (A) chlorate (75 mM) for 48 h at 37 °C. 1 mM PAO was added for 20 min, to inhibit internalization of bFGF prior to initiating the binding reaction. ^{125}I -bFGF was then added to cells at a final concentration of 0.28 nM, and cells were incubated for the indicated times at 37 °C, until steady state was reached. Receptor-bound ^{125}I -bFGF was determined as described (see Materials and Methods). The results presented represent the average \pm SE of triplicate determinations. Rate constants were determined, through computer simulation, by fitting experimental data to produce a theoretical isotherm (line shown). For native cells, the kinetic constants are $k_{\text{on}} = 1.2 \times 10^8 \text{ M}^{-1} \text{ min}^{-1}$ and $k_{\text{off}} = 0.038 \text{ min}^{-1}$; and for chlorate-treated cells, $k_{\text{on}} = 4.2 \times 10^8 \text{ M}^{-1} \text{ min}^{-1}$ and $k_{\text{off}} = 0.79 \text{ min}^{-1}$.

Table 2: Kinetic Constants for bFGF Binding and Degradation in Native and Chlorate-Treated VSMC

constants	native	chlorate treated
$k_{\text{on}} (\text{M}^{-1} \text{ min}^{-1})$	1.2×10^8	4.2×10^8
$k_{\text{off}} (\text{min}^{-1})$	0.038	0.79
$K_d (\text{nM})$	0.32	1.9
$k_{\text{deg}} (\text{min}^{-1})$	5.6×10^{-3}	20.0×10^{-3}

^a The results of the receptor binding studies (Figure 1), along with data for the amounts of bFGF in the media and bound to HSPG sites on the cell surface (data not shown, defined by eqs 1–3), were entered in the computer simulation which minimized the difference between the model and the data. Apparent degradation rate constants were determined analytically (see eq 6) using the data presented in Figure 10A along with data for the internalized ^{125}I -bFGF fraction from this study (data not shown).

HSPG-deficient conditions results in an identical decrease in sensitivity to bFGF-stimulated mitogenesis. While the dose response curve for chlorate-treated Balb/c3T3 cells for stimulation of DNA synthesis was shifted by approximately 1 order of magnitude, the maximal response was identical

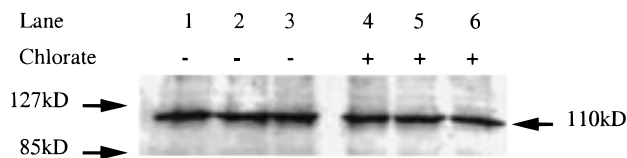


FIGURE 2: Immunoblot analysis of FGF receptor 1 levels in native and HSPG-deficient VSMC. VSMC were treated with (+) or without (–) chlorate (75 mM) for 48 h at 37 °C. After chlorate treatment, cells were extracted, subjected to 5% SDS–PAGE, and transferred to Immobilon-P membranes. Membranes were hybridized with an anti-FGF receptor 1 antibody followed by horseradish peroxidase-conjugated anti-IgG. Bands were visualized using enhanced chemiluminescence. A single prominent band was observed with an apparent molecular mass of 110 kDa.

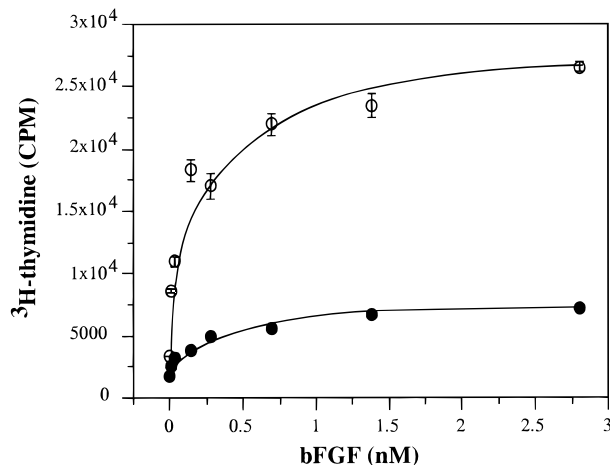


FIGURE 3: Stimulation of DNA synthesis in native and HSPG-deficient VSMC. VSMC were treated with (●) or without (○) chlorate (75 mM) for 48 h at 37 °C. The indicated concentrations of bFGF were added along with [³H]thymidine (1 μCi/mL), and cells were incubated for 48 h at 37 °C. Cells were fixed with methanol, DNA was precipitated with TCA, and radioactivity was measured in a scintillation counter. The results presented represent the average ± SE of triplicate determinations.

to that for native cells (38). To determine if the altered bFGF binding kinetics in chlorate-treated cells result in a change in bFGF response, bFGF stimulation of DNA synthesis was evaluated in native and chlorate-treated cells (Figure 3). Chlorate-treated cells showed significantly decreased [³H]-thymidine incorporation at all doses of bFGF as compared to native VSMC. The maximal response of chlorate-treated cells to bFGF was only 20% of the native response. The decreased responsiveness to bFGF was not simply an artifact of chlorate treatment, as chlorate-treated cells responded as well as native cells to serum or a non-HSPG-binding growth factor such as epidermal growth factor (EGF) (Table 3). The decreased responsiveness of chlorate-treated VSMC to bFGF is not fully accounted for by the decreased receptor affinity. At concentrations of bFGF where native and chlorate-treated cells bind similar amounts of bFGF, based on the receptor K_d 's (Table 2), the native cells showed a 3–4-fold greater response (Figures 3 and 4). For example, at the lowest bFGF concentration used (13.8 pM), only 4% of the available receptors on the native cells would be predicted to be bound, yet the stimulation of DNA synthesis was almost equal to that observed in chlorate-treated cells treated with 2.8 nM bFGF where 60% of the receptors are predicted to be bound (Figure 4). The difference in the mitogenic responsiveness under these two conditions does not appear to reflect an alter-

Table 3: Stimulation of DNA Synthesis by EGF and Calf Serum in Native and Chlorate-Treated Cells^a

treatment	native (cpm)	chlorate treated (cpm)
no addition	16874 ± 764	23309 ± 9274
EGF (0.8 nM)	179004 ± 7519	139837 ± 11456
calf serum (10%)	175012 ± 4702	267066 ± 49856

^a VSMC were treated with or without chlorate (75 mM) for 48 h at 37 °C. EGF or calf serum was added along with [³H]thymidine (1 μCi/mL), and cells were incubated for 48 h at 37 °C. Cells were fixed with methanol, DNA was precipitated with TCA, and radioactivity was measured in a scintillation counter. The results presented represent the average ± SE of triplicate determinations.

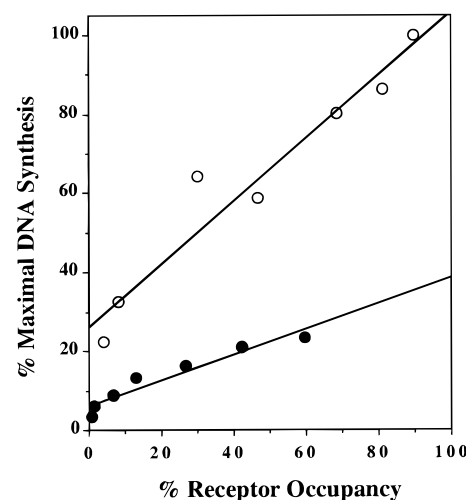


FIGURE 4: Correlation between FGF receptor occupancy and stimulation of DNA synthesis by bFGF in native and chlorate-treated VSMC. The percent maximal DNA synthesis stimulatory activity of bFGF (Figure 3) was determined relative to the maximal [³H]thymidine incorporation in native cells (100%). The percent receptor occupancy was determined for native (○) and chlorate-treated (●) cells using the K_d 's determined in Figure 1 (Table 2) and the following relationship: % receptor occupancy = $[\text{bFGF}] / (K_d + [\text{bFGF}]) \times 100$. Receptor binding correlated with activity for both native and chlorate-treated cells ($R^2 = 0.938$ and 0.923 for native and chlorate-treated cells, respectively). However, the relationship between binding and activity under the two conditions was significantly different over the range of bFGF concentrations used (slope = 0.8 and 0.3 for native and chlorate-treated cells, respectively).

ation in cell cycle entry kinetics, as longer or shorter labeling periods with [³H]thymidine did not reveal significantly different results (data not shown). Together these results suggest that HSPG modulate bFGF activity within VSMC at stages in addition to the initial receptor binding event.

HSPG Control the Intracellular Distribution of Internalized bFGF in VSMC. To determine if HSPG are playing a role in modulating the bFGF pathway at stages after receptor binding, the intracellular localization of internalized bFGF within cytoplasmic and nuclear fractions was compared in native and chlorate-treated cells. Cells were incubated with ¹²⁵I-bFGF for 6 h at 37 °C; then the cell surface bound ¹²⁵I-bFGF was removed (high ionic strength, low-pH wash), the cells were extracted and fractionated, and samples were subjected to SDS–PAGE to visualize the internal ¹²⁵I-bFGF (Figure 5). A significant difference in the relative distribution of bFGF was observed in native and chlorate-treated VSMC. While significant ¹²⁵I-bFGF was present in the cytoplasmic fractions for both conditions, significant amounts of ¹²⁵I-bFGF in the nuclear fraction were observed only in

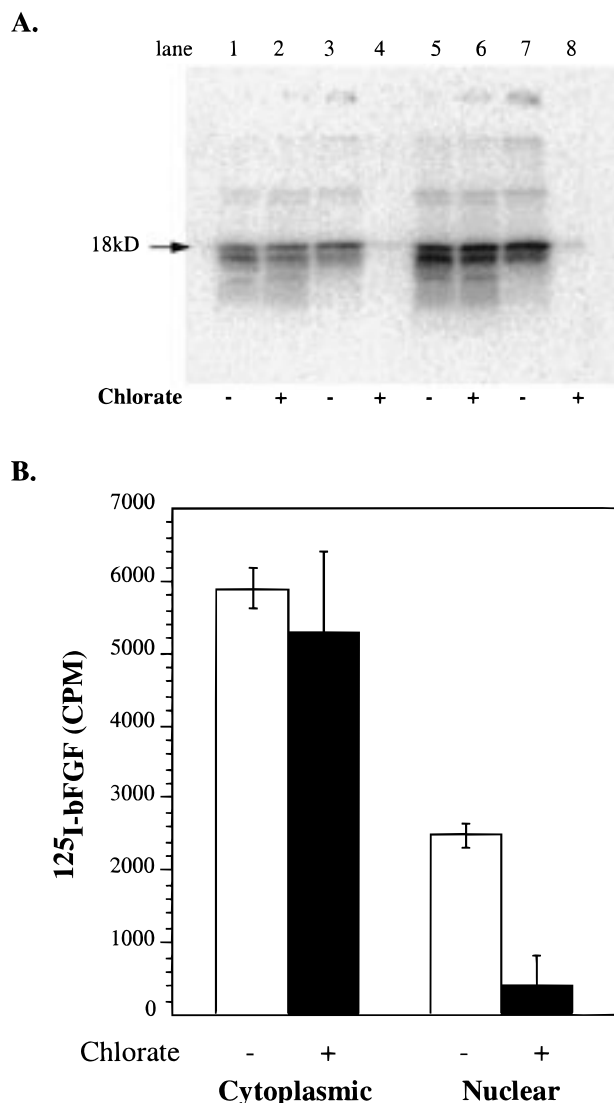


FIGURE 5: Differential localization of bFGF in cytoplasmic and nuclear fractions of native and HSPG-deficient VSMC. VSMC were treated with (+) or without (-) chlorate (75 mM) for 48 h at 37 °C. ¹²⁵I-bFGF was then added to cells at a final concentration of 0.28 nM (lanes 1–4) or 0.56 nM (lanes 5–8), and cells were incubated for 6 h at 37 °C. ¹²⁵I-bFGF was extracted and quantitated by gamma counting from cytoplasmic (lanes 1, 2, 5, and 6) and nuclear (lanes 3, 4, 7, and 8) fractions as described (see Materials and Methods) and applied to a 16% SDS–PAGE. The gel was dried and exposed to a phosphorimager plate for 5 days. (A) Bands were visualized using a phosphorimager. (B) Quantitation of ¹²⁵I-bFGF in each sample treated with 0.56 nM ¹²⁵I-bFGF is presented as the average \pm SE of triplicate determinations.

native cells. The effects of chlorate treatment on bFGF localization were reversible, indicating that chlorate treatment did not cause a permanent disruption in the bFGF processing machinery in these cells. Chlorate was removed from chlorate-treated VSMC, and the cells were allowed to recover for 48 h then exposed to ¹²⁵I-bFGF followed by fractionation. There was no significant change in the incorporation of ¹²⁵I-bFGF in the cytoplasmic fraction; however, the ability to accumulate bFGF within the nuclear fraction had substantially recovered, to near control levels, in the chlorate-pre-treated cells (data not shown).

Since there were similar amounts of bFGF in the cytoplasmic fractions from native and chlorate-treated cells, the

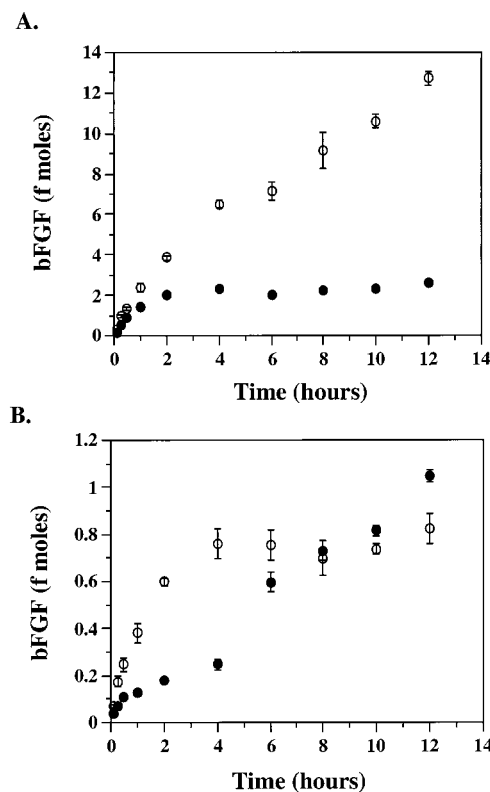


FIGURE 6: Time course of cellular localization of bFGF in native and HSPG-deficient VSMC. VSMC were treated with (●) or without (○) chlorate (75 mM) for 48 h at 37 °C. ¹²⁵I-bFGF was then added to cells at a final concentration of 0.28 nM, and cells were incubated for indicated times at 37 °C. At each time point, cell surface bound bFGF was removed, and cells were extracted and fractionated into cytoplasmic and nuclear pools. ¹²⁵I-bFGF was extracted from cytoplasmic fractions (A), and from nuclear fractions (B) for quantitation as described (see Materials and Methods). The results presented represent the average \pm SE of triplicate determinations.

decreased nuclear localization in the chlorate-treated cells was not simply a consequence of decreased surface binding. The SDS–PAGE analyses also revealed the presence of bFGF degradation products in the cytoplasmic fractions. No significant degradation products were observed within the nuclear fractions. These results suggest that localization of bFGF to the nuclear fraction might be accompanied by decreased degradation.

To determine the level at which HSPG is involved in modulating bFGF intracellular localization, the kinetics of these processes were measured in native and chlorate-treated cells. The accumulation of bFGF within the cytoplasmic fraction occurred at similar initial rates in native and chlorate-treated cells (Figure 6A). However, native VSMC were able to maintain a nearly linear rate of bFGF incorporation throughout the time course, while cytoplasmic accumulation reached a steady state after 3–4 h in chlorate-treated cells. The kinetic profile for bFGF in the nuclear fraction was significantly different than the cytoplasmic fraction. Whereas native VSMC approached steady state in the nuclear fraction at a faster rate, and incorporated high levels of bFGF rapidly, chlorate-treated VSMC showed a slower steady rate of nuclear incorporation of bFGF (Figure 6B). The distinctions between native and chlorate-treated VSMC, and between the cytoplasmic and nuclear fractions, were consistent over a large number of experiments using various bFGF concentra-

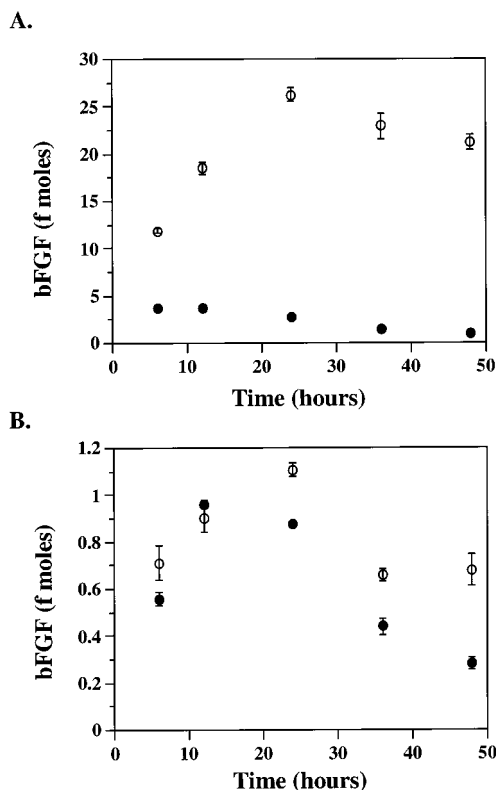


FIGURE 7: Long-term time course of cellular localization of bFGF in native and HSPG-deficient VSMC. VSMC were treated with (●) or without (○) chlorate (75 mM) for 48 h at 37 °C. ^{125}I -bFGF (0.28 nM) was added to cells and the incubation continued for the indicated times at 37 °C. Cells were washed and ^{125}I -bFGF extracted as described in Figure 6. Cytoplasmic ^{125}I -bFGF (A); nuclear ^{125}I -bFGF (B). The results presented represent the average \pm SE of triplicate determinations.

tions with cells from several separate isolations. However, we did note quantitative differences in the kinetic profiles from one experiment to another. For example, the length of time after which the cytoplasmic accumulation in native and chlorate-treated cells began to deviate from one another ranged from 2 to 6 h. The point where the nuclear accumulation in native and chlorate-treated VSMC became similar was found to vary from 6 to 12 h, and in some instances, the amount of bFGF in the nuclei of chlorate-treated cells never reached that of the native at any time point measured.

Longer term experiments were also conducted to determine if the accumulation of bFGF in the cytoplasmic fraction in native cells and the nuclear fraction in chlorate-treated cells is subject to saturation (Figure 7). Cytoplasmic bFGF continued to accumulate in native cells, increasing $\sim 40\%$ from 12 to 24 h, and was followed by an $\sim 20\%$ decline from 24 to 48 h. In chlorate-treated cells, cytoplasmic bFGF was unchanged from 2 to 12 h and then showed a steady $\sim 70\%$ decline up to 48 h. The amount of nuclear bFGF remained unchanged in native and chlorate-treated cells from 12 to 24 h, after which a steady $\sim 50\%$ decline was observed over the next 24 h. Thus, native cells showed accelerated nuclear uptake kinetics and a higher capacity for cytoplasmic bFGF compared to HSPG-deficient VSMC (Figures 6 and 7).

To confirm that the analyses of radioactivity in the intracellular fractions were indicative of the presence of ^{125}I -bFGF and were not significantly weighted by dissociated ^{125}I within the intracellular fractions, trichloroacetic acid (TCA) pre-

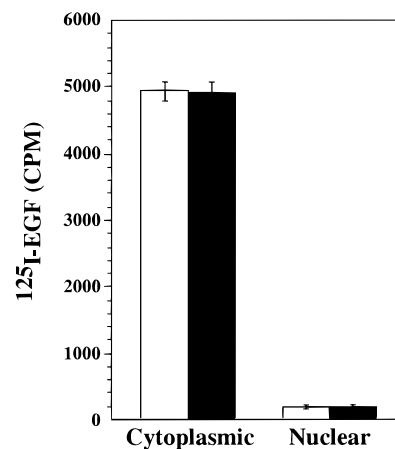


FIGURE 8: EGF localization in cytoplasmic and nuclear fractions of native and HSPG-deficient VSMC. VSMC were treated with (■) or without (□) chlorate (75 mM) for 48 h at 37 °C. ^{125}I -EGF was added to cells at a final concentration of 3.3 ng/mL, and cells were incubated for 3 h at 37 °C. ^{125}I -EGF was extracted from cytoplasmic and nuclear fractions as described (see Materials and Methods) and radioactivity was measured in a gamma counter. The results presented represent the average \pm SE of triplicate determinations.

cipitation was performed. TCA precipitation indicated that 95.1–97.2% of the cytoplasmic and 97.0–99.0% of the nuclear ^{125}I remained incorporated in protein over the time course of these studies. Thus, the TCA-soluble degradation products of bFGF, which are observed in the incubation media, are apparently rapidly exported once generated within the cell.

To ensure that the effects of chlorate on bFGF internalization and intracellular localization were related to the loss of HSPG and not a general effect of chlorate, ^{125}I -EGF localization within native and chlorate-treated VSMC was evaluated. Chlorate had no effect on the cellular accumulation of EGF. A similar amount of EGF accumulated in the cytoplasm of native and chlorate-treated VSMC. Furthermore, there was no significant incorporation of this growth factor in the nuclear fraction of either native or chlorate-treated cells (Figure 8). The lack of EGF within the nucleus even in the presence of high cytoplasmic levels helps confirm the integrity of the fractionation method used since EGF is not believed to be translocated to the nucleus in VSMC. As an additional control, we also conducted Western blot analyses for proliferating cell nuclear antigen (PCNA) on cytoplasmic and nuclear fractions from quiescent and exponentially proliferating VSMC. PCNA was only observed in the nuclear fraction of growing cells, even though it was present in the cytoplasmic fractions of both quiescent and growing VSMC (data not shown). Thus, the bFGF observed within the nuclear fraction is not simply a consequence of cytoplasmic contamination.

bFGF Degradation Is Increased in HSPG-Deficient VSMC. The increased accumulation of bFGF in the cytoplasmic fraction of native compared to chlorate-treated cells after long incubation periods could be the result of increased uptake of bFGF from the cell surface or decreased clearance of bFGF. Pulse–chase experiments were conducted to determine the bFGF clearance rates in native and chlorate-treated cells. Cells were incubated with ^{125}I -bFGF for a period of 9 h to allow for significant cytoplasmic accumulation of ^{125}I -

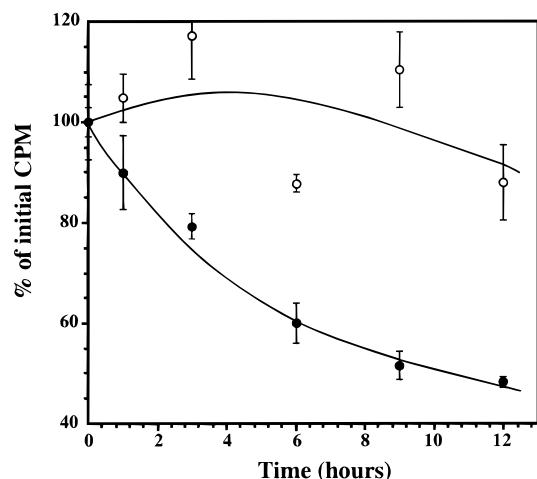


FIGURE 9: Intracellular bFGF clearance kinetics in native and HSPG-deficient VSMC. VSMC were treated with (●) or without (○) chlorate (75 mM) for 48 h at 37 °C. ^{125}I -bFGF was then added to cells at a final concentration of 0.28 nM, and the cells were incubated for 9 h at 37 °C (pulse), to allow for ^{125}I -bFGF internalization. After this time, cells were washed with binding buffer and high-salt, low-pH buffer (see Materials and Methods), to remove all soluble and cell-bound ^{125}I -bFGF. Medium was added back to the cells together with unlabeled bFGF at a final concentration of 0.28 nM (chase). Cells were incubated for the indicated times at 37 °C. Cytoplasmic fractions were isolated, and radioactivity was measured in a gamma counter. The results presented represent the average \pm SE of triplicate determinations.

bFGF (pulse period). After this pulse period, the ^{125}I -bFGF-containing medium was removed, the cells were washed to remove all surface-bound ^{125}I -bFGF, and the cells were incubated for various times (chase period) in medium containing unlabeled bFGF (0.28 nM). At each chase point, the amount of cytoplasmic ^{125}I -bFGF was measured. A significant difference in clearance was observed in native and chlorate-treated cells. While a large amount (80%) of the cytoplasmic bFGF was lost in chlorate-treated cells over the chase period, only a minimal amount of bFGF was lost from the native VSMC (Figure 9). Estimates of the observed clearance rates indicate that HSPG prolonged the cytoplasmic lifetime of bFGF \sim 8-fold.

The increase in the apparent stability of cytoplasmic bFGF in native cells as compared to chlorate-treated cells may result from decreased bFGF degradation. It is known that a portion of internalized growth factors are degraded in lysosomes. To assess the bFGF degradation rates in cells in the presence and absence of HSPG, we carried out TCA precipitation of the incubation media from native and chlorate-treated VSMC at various times, normalized to the amount of internal bFGF (Figure 10A, see eqs 4–6). The accumulation of TCA-soluble radioactivity in the media fraction of both native and HSPG-deficient VSMC were similar, yet chlorate-treated cells contained significantly less internal bFGF under these conditions. Apparent degradation rate constants (k_{deg}) calculated from these data reveal much higher rates of bFGF degradation within the chlorate-treated cells compared to the native. We find that the k_{deg} for native VSMC was $5.6 (\pm 0.8) \times 10^{-3} \text{ min}^{-1}$, whereas that for chlorate-treated VSMC was $20.0 (\pm 1.5) \times 10^{-3} \text{ min}^{-1}$. To determine if the increased uptake of bFGF in native VSMC was simply saturating a degradatory pathway, we exposed native and chlorate-treated VSMC to increased doses of bFGF and

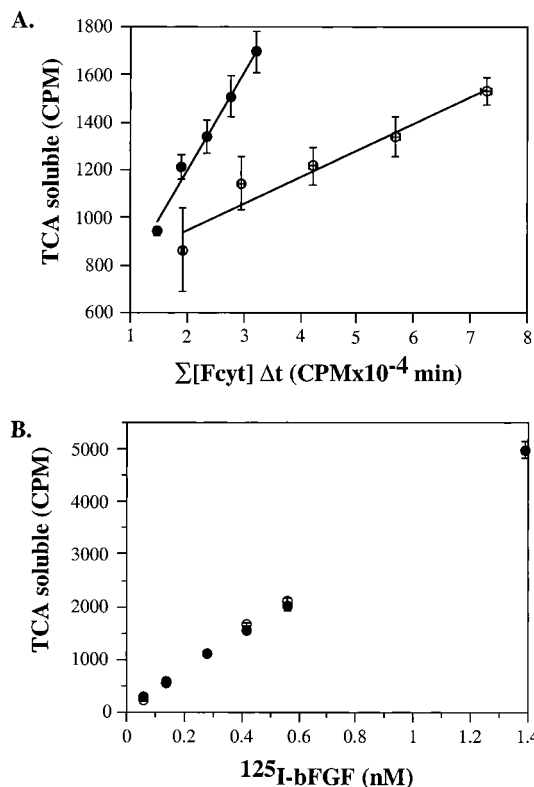


FIGURE 10: bFGF degradation kinetics in native and HSPG-deficient VSMC. VSMC were treated with (●) or without (○) chlorate (75 mM) for 48 h at 37 °C. (A) ^{125}I -bFGF was added to cells at a final concentration of 0.28 nM, and cells were incubated for the indicated times at 37 °C. Medium was collected and subjected to TCA precipitation and the internal ^{125}I -bFGF extracted and quantitated as described (see Materials and Methods). The results presented represent the amount of TCA soluble (degraded) ^{125}I -bFGF in the culture medium plotted against the sum of the internal fraction at each time point (see eqs 4–6). (B) ^{125}I -bFGF was added at the indicated concentrations, and the cells were incubated for 2 h at 37 °C. Medium was collected and subjected to TCA precipitation, and the amount of soluble radioactivity is presented as degraded bFGF. The results presented represent the average \pm SE of triplicate determinations.

measured the amount of TCA-soluble bFGF degradation products in the media (Figure 10B). We found that the amount of bFGF degraded increased linearly over this range of bFGF concentrations, suggesting that the degradation pathway is not nearing saturation under these conditions. Furthermore, the amount of degraded material in the media remained the same for both native and HSPG-deficient VSMC over this range of bFGF concentrations. Thus, decreased degradation appears to be one factor contributing to the altered intracellular distribution and lifetime of bFGF in cells that contain HSPG compared to HSPG-deficient cells.

DISCUSSION

Heparan sulfate proteoglycans have been known to modulate the activity of bFGF both in the extracellular environment, by maintaining large reservoirs of active bFGF, and on the cell surface, by increasing the affinity of bFGF for its receptors [(10, 18) for review]. The presence of HSPG at the cell surface has also been suggested to affect bFGF trafficking events, such as internalization and localization (25, 34, 36, 37). We have investigated the role of HSPG in modulating the bFGF pathway after initial binding to

receptors in VSMC. While we and others have shown that the effects of HSPG on bFGF activity can be attributed to altered surface binding in some instances (38, 60), we show here that the ability of bFGF to stimulate DNA synthesis in HSPG-deficient VSMC was not recovered to native levels in the presence of high bFGF concentrations (Figure 3). The decreased mitogenic activity of bFGF in HSPG-deficient VSMC might relate to altered intracellular trafficking and degradation of bFGF within these cells (Figures 5–7, 9, 10). We observed a reduced initial rate of bFGF accumulation within the nuclear fraction of chlorate-treated cells compared to native cells during the first 0–6 h of bFGF treatment (Figures 5–7). We also observed that intracellular bFGF had a significantly prolonged lifetime in cells that contain HSPG compared to chlorate-treated cells, in part, because of reduced degradation rates (Figures 9 and 10, and Table 2). Thus, critical functions of HSPG in VSMC might involve the protection of intracellular bFGF from degradation and rapid nuclear incorporation during a limited period of time after initial FGF receptor engagement and activation. Precise coordination of the sequence and timing of a series of growth factor induced events within a target cell might be necessary for an end point biological response such as mitogenesis. Furthermore, this type of complex cellular instruction system could also provide for a wide range of distinct biological activities induced by a single growth factor determined by the combined presence of a number of intersecting pathways.

Many previous studies with bFGF and other growth factors have indicated that growth factor induced mitogenesis often appears to involve events that occur after receptor internalization. Activation of FGF receptors on the cell surface results in rapid and transient activation of the intrinsic receptor tyrosine kinase and phospholipase C- γ , followed by activation of the mitogen-activated protein kinase pathway (8, 61). While some of these events appear to be necessary for bFGF-mediated stimulation of cell proliferation, significant data exist suggesting that additional bFGF-mediated events are also required. Since the half-life of bFGF inside the cell is unusually long (18–24 h) compared to other growth factors, such as EGF which has an intracellular half-life on the order of 10–20 min, it is possible that bFGF and its receptors play important intracellular roles. Indeed, intracellular loops for growth factors have long been postulated to provide a mechanism for autocrine stimulation. The bFGF gene lacks a conventional signal sequence for secretion (62), and endogenous bFGF often accumulates within cytoplasmic and nuclear regions of producing cells (63–66). NIH-3T3 cells expressing a bFGF gene containing a fused signal sequence were transformed, yet secreted no detectable bFGF (67). Further, transformation of these cells could be reversed by suramin, which disrupts growth factor receptor complexes, suggesting that the endogenous bFGF was actively stimulating the cells through intracellular receptor complexes (68). In addition to these observations, studies conducted using toxin-fused FGFs, mutant receptors, and fibroblast variants have indicated that FGF–receptor complexes need to be internalized and FGF localized to the nucleus in order for FGF to stimulate mitogenesis (69–72).

Localization of growth factors and their receptors to the nuclear region of cells has been an area of intense recent study [see (73) for review]. While a large number of approaches have been employed to demonstrate that exog-

enous and endogenous aFGF and bFGF are able to partition into the nuclei in a variety of cell types, this process has been less well characterized for other ligands. Evidence exists that interleukin 1, a ligand that like FGF remains within cells for prolonged periods ($t_{1/2} \sim 8$ h), also accumulates within nuclear fractions (74–76). In addition, there is evidence that EGF, insulin, nerve growth factor, platelet-derived growth factor, and the receptors for these ligands are localized to, or associated with, the nucleus in some cell systems (77–79). However, definitive nuclear localization of some of these ligands and receptors awaits confirmation. The function of nuclear accumulation of growth factors and/or their receptors remains unclear. FGF has been proposed to regulate gene expression through direct interaction with DNA [see (73) for review]. It has also been demonstrated that bFGF binds the protein kinase CK2 and stimulates its activity toward nucleolin, a natural substrate found in the nucleus (69). The interaction of bFGF with CK2 was correlated with mitogenic activity. Nuclear-associated FGF-R1 tyrosine kinase activity has also been detected in aFGF-treated Balb/c3T3 cells during the entire G1 period of the cell cycle (12). These studies, together with the data presented here, suggest that bFGF and its receptors might have functions that depend on their subcellular localization during specific periods within the cell cycle. Furthermore, our studies indicate that the HSPG coreceptors for bFGF might play critical functions in controlling the kinetics and distribution of bFGF within cells. More detailed kinetic analyses of these processes will need to be conducted to clearly identify the relationship of cellular response to quantitative differences in the kinetics of these intracellular growth factor trafficking events.

We found significantly decreased nuclear accumulation of bFGF in HSPG-deficient VSMC during the first several hours of treatment, as compared to native cells (Figures 5–7). This difference was not simply a consequence of decreased cell surface binding of bFGF since, under these conditions, the differences between surface-bound and cytoplasmic bFGF in native and HSPG-deficient cells were much less pronounced than for the nuclear fractions. Thus, HSPG appear to initially play a selective function at directing bFGF to the nucleus in VSMC. However, it is important to note that at later time points, the relative amount of nuclear bFGF in HSPG-deficient cells is greater than that in native cells. This could be, in part, the result of the potential presence of saturable bFGF binding sites on or in the nucleus. In native cells, these sites might become rapidly saturated (2–4 h) such that the continued accumulation of cytoplasmic bFGF does not result in increased nuclear bFGF, while in chlorate-treated cells this process is delayed (8–12 h). These possibilities as well as the biological/biochemical significance of the altered rates of nuclear accumulation await further experimentation.

It is possible that the increased nuclear localization of bFGF in native cells is a consequence of increased stability of intracellular bFGF–receptor complexes. The ability of HSPG to stabilize bFGF–receptor binding, reflected by a 20-fold decrease in the apparent off rate constant for bFGF–receptor complexes on native cells as compared to HSPG-deficient cells (Figure 1 and Table 2), might limit dissociation of bFGF within endosomal compartments, preventing eventual lysosomal degradation. Furthermore, high-affinity ter-

nary complexes, involving bFGF simultaneously bound to its receptor and HSPG, generated on the cell surface of native cells, unlike binary bFGF–receptor complexes, would be resistant to disruption by the low-pH environments encountered in intracellular endosomal compartments (19, 38, 80). Mechanisms might also involve partial degradation of HSPG in lysosomes, releasing soluble bFGF–heparan sulfate complexes that could have unique trafficking properties within cells. Hence, the effects of HSPG on the kinetics and nature of bFGF–receptor interactions that we and others have detailed might have extended consequences inside the cell after receptor internalization. Indeed, alterations in the pH sensitivity of ligand–receptor interactions have been demonstrated to affect ligand trafficking and activity with EGF family growth factors (55). Alternatively, the well-known ability of HSPG to physically protect bFGF from proteolytic degradation (81, 82) could be involved in slowing bFGF degradation within native VSMC. Together these events might increase the effective lifetime of a signaling bFGF–receptor complex within the cell, leading to the generation of a critical level of signal required to induce mitogenesis.

While the quantitative effects of HSPG on the kinetics of bFGF binding and processing might be sufficient to explain the qualitative differences in mitogenic responsiveness of native and HSPG-deficient VSMC, it is also likely that specific HSPG species present on VSMC have unique functions within the bFGF pathway. For instance, information might reside within the core protein of a cell surface HSPG that targets it and its ligand to the nucleus. In the present study, we have analyzed bFGF binding and processing in native (containing the full range of HSPG) and HSPG-deficient (chlorate-treated cells containing non-sulfate proteoglycan) VSMC. A more selective analysis is required to identify the functions of each individual HSPG. It is interesting to note that the selective effects of HSPG on nuclear accumulation of bFGF were not observed in Balb/c3T3 or bovine aortic endothelial cells (data not shown). Mitogenic stimulation by bFGF in these cell types, in HSPG-deficient states, was fully recoverable to the levels observed for the native cells. These results suggest that levels of control might exist for bFGF in some cell types but not others. Cell type distinctions might be related to differential expression of particular HSPG species.

Our analysis of the kinetics of the intracellular processing of bFGF revealed a complex series of interrelated events. In the cytoplasmic fraction, native VSMC accumulate bFGF linearly for over 12 h, whereas HSPG-deficient cells reach a rapid steady state (2–4 h) after which the levels of ¹²⁵I-bFGF are unaltered. In the nuclear fraction, the inverse occurs; native VSMC incorporate bFGF rapidly and reach steady state sooner (4–6 h), whereas HSPG-deficient VSMC incorporate bFGF slower over a prolonged period (12 h). The clearance rate of cytoplasmic ¹²⁵I-bFGF was much slower for native than for HSPG-deficient VSMC, in part, as a result of decreased degradation. The biochemical and biological consequences of these differences have not been fully defined. However, these studies demonstrate that kinetic differences exist in the bFGF intracellular processing pathway in native and HSPG-deficient VSMC. These kinetic differences might reflect significant alterations in the bFGF pathway that are critical in directing the response of VSMC to bFGF. These studies imply that one mode of regulation

which cells use to distinguish between various growth factors, that activate similar signaling pathways, may rely on the timing and extent to which these pathways are activated. Also, these studies add to the growing evidence that not only cell surface events are important in governing the cellular response to growth factors, but also downstream intracellular events are activated by the initial ligand receptor interaction.

In conclusion, we have shown that the VSMC response to bFGF correlated with the ability of these cells to rapidly accumulate bFGF within nuclear fractions and stabilize cytoplasmic bFGF against degradation. The ability to rapidly accumulate nuclear bFGF was dependent on the cellular expression of HSPG. Thus, a function of HSPG in VSMC might be to direct the intracellular trafficking of bFGF which could dictate the eventual cellular response. These results suggest that VSMC might be extremely sensitive to growth modulation by heparin and heparin binding growth factors as the result of the presence of a multilayered system of control. It will be important to determine the nature and function of individual proteoglycan species on VSMC. Furthermore, it is possible that HSPG function as general modulators of the intracellular trafficking for the large family of heparin binding growth factors in VSMC. Understanding how the particular composition of the cell surface modulates intracellular events, and ultimately the cellular response to mitogenic factors, might provide important insight into the rational design of new therapies aimed at selectively modulating cell proliferation.

ACKNOWLEDGMENT

We thank Jo Ann Buczek-Thomas for her critical review of the manuscript. We are grateful to Jeffrey Sperinde for advice in optimizing the computer simulation program.

REFERENCES

1. Bikfalvi, A., Klein, S., Pintucci, G., and Rifkin, D. B. (1997) *Endocr. Rev.* 18, 26–45.
2. Murphy, M., Drago, J., and Bartlett, P. F. (1990) *J. Neurosci. Res.* 25, 463–475.
3. Olwin, B. B., Arthur, K., Hannon, K., Hein, P., McFall, A., Riley, B., Szebenyi, G., Zhou, Z., Zuber, M. E., Rapraeger, A. C., et al. (1994) *Mol. Reprod. Dev.* 39, 90–100.
4. Klagsbrun, M., and Edelman, E. R. (1989) *Arteriosclerosis* 9, 269–278.
5. Cascells, W. (1991) *J. Cell. Biochem.* 15C, 98.
6. Lindner, V., Lappi, D. A., Baird, A., Majack, R. A., and Reidy, M. A. (1991) *Circ. Res.* 68, 106–113.
7. Edelman, E. R., Nugent, M. A., Smith, L. T., and Karnovsky, M. J. (1992) *J. Clin. Invest.* 89, 465–473.
8. Jaye, M., Schlessinger, J., and Dionne, C. A. (1992) *Biochim. Biophys. Acta* 1135, 185–199.
9. Johnson, D. E., and Williams, L. T. (1993) *Adv. Cancer Res.* 60, 1–41.
10. Turnbull, J. E., and Gallagher, J. T. (1993) *Biochem. Soc. Trans.* 21, 477–482.
11. Maher, P. A. (1996) *J. Cell Biol.* 134, 529–536.
12. Prudovsky, I., Savion, N., Zhan, X., Friesel, R., Xu, J., Hou, J., McKeenan, W. L., and Maciag, T. (1994) *J. Biol. Chem.* 269, 31720–31724.
13. Kjell  n, L., and Lindahl, U. (1991) *Annu. Rev. Biochem.* 60, 443–475.
14. Turnbull, J. E., Fernig, D. G., Ke, Y., Wilkinson, M. C., and Gallagher, J. T. (1992) *J. Biol. Chem.* 267, 10337–10341.
15. Guimond, S., Maccarana, M., Olwin, B. B., Lindahl, U., and Rapraeger, A. C. (1993) *J. Biol. Chem.* 268, 23906–23914.

16. Krufka, A., Guimond, S., and Rapraeger, A. C. (1996) *Biochemistry* 35, 11131.
17. Logan, A., and Hill, D. J. (1992) *J. Endocrinol.* 134, 157–161.
18. Schlessinger, J., Lax, I., and Lemmon, M. (1995) *Cell* 83, 357–360.
19. Nugent, M. A., and Edelman, E. R. (1992) *Biochemistry* 31, 8876–8883.
20. Ornitz, D. M., Yayon, A., Flanagan, J. G., Svahn, C. M., Levi, E., and Leder, P. (1992) *Mol. Cell. Biol.* 12, 240–247.
21. Rapraeger, A. C. (1995) *Chem. Biol.* 2, 645–649.
22. Forsten, K. E., Courant, N. A., and Nugent, M. A. (1997) *J. Cell. Physiol.* 172, 209–220.
23. Saksela, O., Moscatelli, D., Sommer, A., and Rifkin, D. B. (1988) *J. Cell Biol.* 107, 743–751.
24. Flaumenhaft, R., and Rifkin, D. (1992) *Mol. Biol. Cell* 3, 1057–1065.
25. Reiland, J., and Rapraeger, A. C. (1993) *J. Cell Sci.* 105, 1085–1093.
26. Amalric, F., Baldwin, V., Bosc-Bierne, I., Bugler, B., Couderc, B., Guyader, M., Patry, V., Prats, H., Roman, A. M., and Bouche, G. *Ann. N.Y. Acad. Sci.* 638, 127–138.
27. Amalric, F., Bouche, G., Bonnet, H., Brethenou, P., Roman, A. M., Truchet, I., and Quarto, N. (1994) *Biochem. Pharmacol.* 47, 111–115.
28. Joy, A., Moffett, J., Neary, K., Mordechai, E., Stachowiak, E. K., Coons, S., Rankin-Shapiro, J., Florkiewicz, R. Z., and Stachowiak, M. K. (1997) *Oncogene* 14, 171–183.
29. Hawker, J. R., and Granger, H. J. (1992) *Am. J. Physiol.* 262, H1525–H1537.
30. Speir, E., Sasse, J., Shrivastav, S., and Casscells, W. (1991) *J. Cell. Physiol.* 147, 362–373.
31. Bikfalvi, A., Dupuy, E., Inyang, A. L., Fayein, N., Leseche, G., Courtois, Y., and Tobelem, G. (1989) *Exp. Cell Res.* 181, 75–84.
32. Prudovsky, I. A., Savion, N., LaVallee, T. M., and Maciag, T. (1996) *J. Biol. Chem.* 271, 14198–14205.
33. Stachowiak, M. K., Maher, P. A., Joy, A., Mordechai, E., and Stachowiak, E. K. (1996) *Mol. Brain Res.* 38, 161–165.
34. Rusnati, M., Urbinati, C., and Presta, M. (1993) *J. Cell. Physiol.* 154, 152–161.
35. Moscatelli, D. (1988) *J. Cell Biol.* 107, 753–759.
36. Gannoun-Zaki, L., Pieri, I., Badet, J., Moenner, M., and Barritault, D. (1991) *Exp. Cell Res.* 197, 272–279.
37. Gleizes, P.-E., Noaillac-Depeyre, J., Amalric, F., and Gas, N. (1995) *Eur. J. Cell Biol.* 66, 47–59.
38. Fannon, M., and Nugent, M. A. (1996) *J. Biol. Chem.* 271, 17949–17956.
39. Castellot, J. J., Addonizio, M. L., Rosenberg, R. D., and Karnovsky, M. J. (1981) *J. Cell Biol.* 90, 372–379.
40. Clowes, A. W., and Karnovsky, M. J. (1977) *Nature (London)* 265, 625–626.
41. Fritze, L., Reilly, C., and Rosenberg, R. (1985) *J. Cell Biol.* 100, 1041–1049.
42. Benitz, W. E., and Bernfield, M. (1990) *Am. J. Respir. Cell Mol. Biol.* 2, 407–408.
43. Nugent, M. A., Karnovsky, M. J., and Edelman, E. R. (1993) *Circ. Res.* 73, 1051–1060.
44. Lindner, V., and Reidy, M. A. (1991) *Proc. Natl. Acad. Sci. U.S.A.* 88, 3739–3743.
45. Castellot, J. J., Rosenberg, R. D., and Karnovsky, M. J. (1984) in *Biology of endothelial cells* (Jaffe, E. A., Ed.) pp 118–128, Martinus Nijhoff Publishers, Boston.
46. Vlodavsky, I., Folkman, J., Sullivan, R., Fridman, R., Ishai-Michaeli, R., Sasse, J., and Klagsbrun, M. (1987) *Proc. Natl. Acad. Sci. U.S.A.* 84, 2292–2296.
47. Folkman, J., Klagsbrun, M., Sasse, J., Wadzinski, M., Ingber, D., and Vlodavsky, I. (1988) *Am. J. Pathol.* 130, 393–400.
48. Dodge, A. B., Lu, X., and D'Amore, P. A. (1993) *J. Cell. Biochem.* 53, 21–31.
49. Ross, R. (1971) *J. Cell Biol.* 50, 172–186.
50. Connolly, D. T., Knight, M. B., Harakas, N. K., Wittwer, A. J., and Feder, J. (1986) *Anal. Biochem.* 152, 136–140.
51. Forsten, K. E., and Lauffenburger, D. A. (1992) *Biophys. J.* 61, 1–12.
52. Rapraeger, A., and Yeaman, C. (1989) *Anal. Biochem.* 179, 361–365.
53. Nugent, M. A., and Edelman, E. R. (1992) *J. Biol. Chem.* 267, 21256–21264.
54. Gibson, A. E., Noel, R. J., Herlihy, J. T., and Ward, W. F. (1989) *Am. J. Physiol.* 257, C182–C184.
55. French, A. R., Tadaki, D. K., Niyogi, S. K., and Lauffenburger, D. A. (1995) *J. Biol. Chem.* 270, 4334–4340.
56. Press, W. H., Flannery, B. P., Teukolsky, S. A., and Vetterling, W. T. (1986) *Numerical Recipes*, Cambridge University Press, Cambridge.
57. Baird, A., and Bohlen, P. (1990) in *Peptide Growth Factors and Their Receptors I* (Sporn, M. B., and Roberts, A. B., Eds.) pp 369–418, Springer-Verlag, Berlin and Heidelberg.
58. Rapraeger, A., Krufka, A., and Olwin, B. (1991) *Science* 252, 1705–1708.
59. Aviezer, D., Hecht, D., Safran, M., Eisinger, M., David, G., and Yayon, A. (1994) *Cell* 79, 1005–1013.
60. Roghani, M., Mansukhani, A., Dell'Era, P., Bellosta, P., Basilico, C., Rifkin, D. B., and Moscatelli, D. (1994) *J. Biol. Chem.* 269, 3976–3984.
61. Friesel, R. E., and Maciag, T. (1995) *FASEB J.* 9, 919–925.
62. Abraham, J. A., Mergia, A., Whang, J. L., Tuomolo, A., Friedman, J., Hjerrild, K. A., Gospodarowicz, D., and Fiddes, J. C. (1986) *Science* 233, 545–548.
63. Tessler, S., and Neufeld, G. (1990) *J. Cell. Physiol.* 145, 310–317.
64. Bikfalvi, A., Klein, S., Pintucci, G., Quarto, N., Mignatti, P., and Rifkin, D. B. (1995) *J. Cell Biol.* 129, 233–243.
65. Dell'Era, P., Presta, M., and Ragnotti, G. (1991) *Exp. Cell Res.* 192, 505–510.
66. Renko, M., Quarto, N., Morimoto, T., and Rifkin, D. B. (1990) *J. Cell. Physiol.* 144, 108–114.
67. Rogelj, S., Weinberg, R. A., Flanning, P., and Klagsbrun, M. (1988) *Nature* 331, 173–175.
68. Yayon, A., and Klagsbrun, M. (1990) *Proc. Natl. Acad. Sci. U.S.A.* 87, 5346–5350.
69. Bonnet, H., Filhol, O., Truchet, I., Brethenou, P., Cochet, C., Amalric, F., and Bouche, G. (1996) *J. Biol. Chem.* 271, 24781–24787.
70. Mehta, V. B., Connors, L., Wang, H.-C. R., and Chiu, I.-M. (1998) *J. Biol. Chem.* 273, 4197–4205.
71. Lin, Y.-Z., Yao, S., and Hawiger, J. (1996) *J. Biol. Chem.* 271, 5305–5308.
72. Wiedlocha, A., Falnes, P. O., Rapak, A., Munoz, R., Klingenberg, O., and Olsnes, S. (1996) *Mol. Cell. Biol.* 16, 270–280.
73. Hopkins, C. R. (1994) *Biochem. Pharmacol.* 47, 151–154.
74. Grenfell, S., Smithers, N., Miller, K., and Solari, R. (1989) *Biochem. J.* 264, 813–822.
75. Qwarnstrom, E. E., Page, R. C., Gillis, S., and Dower, S. K. (1988) *J. Biol. Chem.* 263, 8261–8269.
76. Mizel, S. B., Kilian, P. L., Lewis, J. C., Paganelli, K. A., and Chizzonite, R. A. (1987) *J. Immunol.* 138, 2906–2912.
77. Podlecki, D. A., Smith, R. M., Kao, M., Tsai, P., Huecksteadt, T., Brandenburg, D., Lasher, R. S., Jarett, L., and Olefsky, J. M. (1987) *J. Biol. Chem.* 262, 3362–3368.
78. Rakowicz-Szulczynska, E. M., Rodeck, U., Herlyn, M., and Koprowski, H. (1986) *Proc. Natl. Acad. Sci. U.S.A.* 83, 3728–3732.
79. Johnson, L. K., Vlodavsky, I., Baxter, J. D., and Gospodarowicz, D. (1980) *Nature* 287, 340–343.
80. Moscatelli, D. (1987) *J. Cell. Physiol.* 131, 123–130.
81. Gospodarowicz, D., and Cheng, J. (1986) *J. Cell. Physiol.* 128, 475–484.
82. Sommer, A., and Rifkin, D. B. (1989) *J. Cell. Physiol.* 138, 215–220.